Glass Struct. Eng.
https://doi.org/10.1007/s40940-020-00130-w

T.I.: PROJECTS & CASE STUDIES

Conceptual design and FEM structural response of a suspended glass sphere made of reinforced curved polygonal panels

Maurizio Froli · Francesco Laccone

Received: 27 April 2020 / Accepted: 5 August 2020

Abstract The paper introduces a novel concept for structural glass shells that is based on the mechanical coupling of double curved heat-bent glass panels and a wire frame mesh, which constitutes a grid of unbonded edge-reinforcement. Additionally, this grid has the purpose of providing redundancy. The panels have load-bearing function, they are clamped at the vertices and dry-assembled. The main novelty lies in the use of polygonal curved panels with a nodal force transfer mechanism. This concept has been validated on an illustrative design case of a 6 m-diameter suspended glass sphere, in which regular pentagonal and hexagonal spherical panels are employed. The good strength and stiffness achieved for this structure is demonstrated by means of local and global FE models. Another fundamental feature of the concept is that the reinforcement grid provides residual strength in the extreme scenarios in which all panels are completely failed. A quantitative measure of redundancy is obtained by comparing this scenario with the ULS.

F. Laccone (✉)
Institute of Information Science and Technologies "Alessandro Faedo" (ISTI), Italian National Research Council (CNR), Via G. Moruzzi 1, 56124 Pisa, Italy
e-mail: francesco.laccone@isti.cnr.it; francesco.laccone@destec.unipi.it

M. Froli · F. Laccone
Department of Energy, Systems, Territory and Construction Engineering, University of Pisa, Largo Lucio Lazzarino 1, 56122 Pisa, Italy
e-mail: m.froli@ing.unipi.it

Keywords Glass shell · Structural glass · Curved glass · Heat bent · Steel reinforcement · Truncated icosahedron · Finite element analysis

1 Introduction

Glass is an ideal material for building skins since it provides for transparency, for resistance to weather phenomena or building separation, and also for load-bearing capacity (Haldimann et al. 2008; Feldmann et al. 2014; Belis et al. 2019). All these capabilities can be simultaneously exploited in building elements such as shear walls and roofs as well as in modern building envelopes where wall and roof elements blend in a single piece. Hence, to maximize the transparency, glass panels are exploited to carry additional loading and not only to support their own weight.

A large topological variety and several structural concepts may be found in building envelopes that behave as a single-layer shells. As almost all the materials used in architecture, glass is produced in flat panels of limited sizes and shapes. These flat panels need to be processed in order to tessellate the ideal shell surface, which is segmented in triangle, quad, diamond or polygonal shapes. The selected discretization strategy has direct implications on the geometry and mechanics of the shell. Thus, the actual structure will result in a faceted surface or possibly the panels can be curved to better approximate the target surface.

Published online: 08 September 2020

However, few glass-covered shells use glass as a structural material, conversely the majority of them are grid shells, in which the metal or timber grid serves as only load-bearing material (Schlaich and Schober 1996; Adriaenssens et al. 2012; Feng and Ge 2013; Bruno et al. 2016; Wang et al. 2016; Mesnil et al. 2017). All these factors make the conceptual design of discrete shells a complex problem.

1.1 Structural glass shells

Similarly to other spatial structures (Romme et al. 2013), structural glass shells can be classified on the basis of their structural behavior. In turn, this latter is affected by the adopted discretization strategy and the joints design.

A first group includes structures based on strut-and-tie or tensegrity behavior. These systems usually adopt triangular or quad panels. Quads are commonly braced by cables to increase the cell stiffness. The panels are point-fixed at their corners, i.e. with clamping. Hence, the structural assembly can be reduced as a discrete system made of axial-only stressed components, similarly to a truss. This behavior is favored by the node transfer mechanism, which causes compression in glass area close to the panels edges that behave as struts, and tension on steel components—if present—that perform as ties. Exemplars of this structures are the post-tensioned dome at Weltbild Verlag building in Augsburg (Wurm 2007) and the Maximilianmuseum roof (Ludwig and Weiler 2000), whose conceptual design has been managed with a reduced truss model. Recently, the work (Laccone et al. 2020) demonstrates how a truss reduced model can be employed to derive the automatic design of strut-and-tie post-tensioned glass shells.

A second group of structural glass shells is based on the shell behavior. These systems manifest surface resistance and rely on continuous smooth load transfer. In fact, the linear joints that are usually adopted to provide for an interrupted force transfer between the panels edges. While for strut-and-tie shells the nodes are vulnerable zones due to high stress, in the shell category stress concentrations are reduced. Again, while for the previous category a mesh with high connectivity (triangle or braced quad) supplies for redundancy; in the shell category, faces with high number of edges have major redundancy. Typically polygonal panels (quads or hexagons) are adopted for the group based of shell behavior. Exemplars of these structures are the Delft dome (Veer et al. 2003), the Blandini's dome (2005; 2008) and the Plate shell structures (Bagger 2010). Recent work demonstrates that a post-tensioned spherical glass shell can span up to 26 m (Hayek et al. 2018).

1.2 Heat-bent curved glass

While flat glass is employed in a significant amount of building applications, bent glass has become more appealing in architectural contexts in which curved forms and continuous reflectivity must be ensured (Neugebauer 2014). Glass can be bent following two main approaches: cold bending, based on forcing and restraining flat panels in situ or during lamination; and heat bending, based on forming new shapes of panels through heating panes up to about 600 °C (Timm and Chase 2014).

The gravity bending or slumping is the traditional and commonly used process for thermally bent glass. It is based on heating a pre-cut flat panel that is laid over a bespoke mould. The high temperature soften the glass while it sinks into the mould due to its own weight. The panels show good optical quality and absence of anisotropies. All shapes from single to double curved are feasible. On the other hand, tempering or heat strengthening process are problematic since they would alter the original forming. So, chemical strengthening and lamination after the bending process are recommended to provide a fail-safe behaviour.

A money-saving process is the online bending, which consists in providing one-axis curvature through a robotic press while the pane is heated in a furnace and pass through it. Apart for time-efficiency, another advantage is that the online bent glass becomes either fully tempered or heat strengthened during the bending process itself.

Thus, while the online bending is used for mass production, the gravity bending ensure the best surface condition and aesthetic quality (Fildhuth et al. 2018). The façade of La Maison des Fondateurs represent an example of using gravity bent glass panels (Villiger et al. 2019). These panels perform as separation walls and as load-bearing elements for both vertical and horizontal forces. In fact, because of the shape stiffness, a curved glass is particularly suitable for application in shell structures.

1.3 Objectives of the present work

Strut-and-tie structures have been already built in large scale exemplars and appear reliable enough since they are tested also in extreme failure scenarios, such as the complete collapse of some panels. On the other hand, the opportunity offered by the shell structure to use polygonal panels is more appealing from an architectural viewpoint because of the reduction of the opaque parts (such as panels edges, seals, reinforcement and nodes) that brings to an increased transparency.

The present work introduces a novel structural concept for glass shells made of polygonal panels that are supported at the vertices and reinforced at the edges by means of unbonded steel rods, combining the features of both categories of structural glass shells. The concept derives from Froli and Laccone (2018), but, apart from the use of curved polygonal panels, it differs from this latter because no post-tensioning is provided as it would lead to a premature buckling failure of curved glass panels.

Reinforcing a tensioned glass panel edge is a commonly-adopted strategy to mitigate the consequences of brittle failures. This steel component is usually bonded or embedded to adhere to glass and to achieve a safer post-cracking phase (Martens et al. 2015a; Louter et al. 2012; Martens et al. 2016; Cupać et al. 2017); the unbonded configuration is more common in post-tensioned glass structures (Froli and Lani 2010; Martens et al. 2015b; Bedon and Louter 2016; Engelmann and Weller 2016). In the present case, dealing with a shell structure, the reinforcement has also a purpose of adding redundancy and avoid global collapse. So, it has to be stiff enough in both tension and compression, and consider the complete failure of panels.

The present concept has been tested on an illustrative case study of a Suspended Glass Sphere (SGS). The structure has been conceived by the author Froli for outdoor use with the aim of hosting a particular art installation in the inside (Fig. 1). It pursues the necessity of guaranteeing an all-round vision of the art object through the transparent and floating envelope, while preserving its functional requirements, such as protection from weather phenomena and accessibility for maintenance.

Although the surface is geometrically defined, its structural behavior is not trivial and presents several complexities given by the positioning of the panels and the response of the whole structure with respect to the suspension system.

Fig. 1 1:10 Scale model demonstrator of the SGS (model by the author Froli)

To state the feasibility of the structure and to validate the structural concept local and global analyses are performed. In the preliminary design phase a reduced model of the glass panels is adopted. Then, detailed local analyses have been performed.

2 Conceptual design and structural system

2.1 Structural concept

The static concept is founded on the collaboration of a wire frame steel structure with spherical bent laminated glass panels (Fig. 2). The steel grid is made of rods that merge in three-way nodes by means of a concentric bolt. Additionally, these nodes are shaped to clamp the vertices of glass panels.

Given these boundary conditions, a nodal load-transfer is expected. Therefore, on a global-level the main loading path is aligned with the edge of the starting mesh and consequently the rods can be either tensioned or compressed. Since the panel corner is not glued but it is simply supported in a dry clamped node, no tension can be transferred to glass. If the ideal edge stretches, tension flows on the rod only; if it shrinks, the rods and the adjacent glass panels work in parallel (Fig. 3).

Apart from aesthetic reasons, the panel double curvature is a local-level strategy to stiffen the glass. Indeed, as long as the nodes are kept in a fixed posi-

Fig. 2 Concept of structural system: bent panels and wire frame steel mesh are connected at the nodes; the panels' edges are then sealed for waterproofing

tion by a polygon of steel rods, the curved glass panel is well supported and can act as a load-bearing shell element. The obtained advantage is to have a stiffer element compared to what it woulve in the case of flat panels. Moreover, the panels are considered as laminated for a safe fail.

The panels vertices are rounded to avoid peak stress concentration and to allow small and reversible displacements under dynamic loads to dissipate energy as performed by Travi Vitree Tensegrity (TVT) prototypes during the experimental tests (Froli and Mamone 2014). Even though the dynamic aspect is not specifically addressed in this work, it is important to see it as part of the conceptual design. The dynamics of glass structures and its interaction with other structural components are becoming an important research topic (Bedon et al. 2018; Bedon and Amadio 2018; Santarsiero et al. 2019; Casagrande et al. 2019).

2.2 Redundancy concept

Redundancy is a fundamental requirement in glass shells (Engelmann et al. 2017) and should consider scenarios in which glass is cracked.

Regarding the geometry, using a polygonal tessellation of the ideal glass surface offers in general a redundant design solution. In fact, in case of glass cracking, having five or six panels in adjacency, alternative load paths may develop. However, a discontinuity on a single node has the effect of weakening the shell behavior. This is the reason why the grid of reinforcement is paramount to avoid these local failures to propagate in global collapses. The grid provides a lower-bound or residual stiffness level.

Evaluating the redundancy from considerations at local level may be very difficult. On the other hand, a more straightforward approach can be adopted considering an extreme failure scenario ('worst case scenario') in which all panels are supposed collapsed (Froli and Laccone 2018). Therefore, collapsed panels are not able to carry shell forces but only to transfer loads to the vertices. This behavior is mechanically akin to a grid shell and can be easily simulated.

2.3 Joint design

The node is the fundamental component of the system since it does accomplish several requirements. The

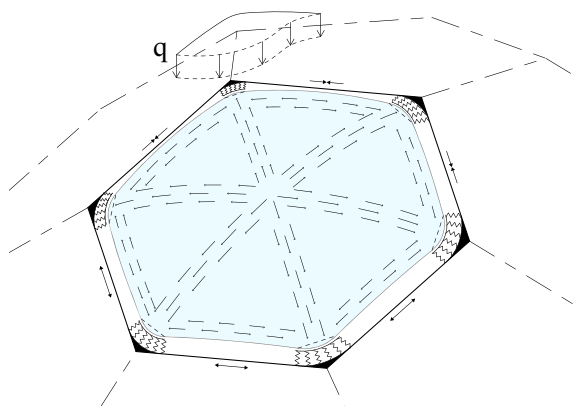

Fig. 3 Free body diagram for the static behavior of reinforced curved polygonal panels

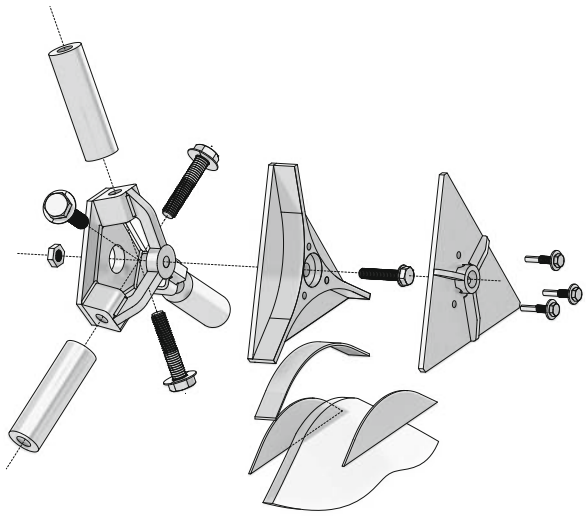

Fig. 4 Conceptual design of the node for the SGS

node is inspired by the TVT nodes (Froli and Mamone 2014), which have been designed for post-tensioned glass beams. A conceptual view of the node designed for the SGS is in Fig. 4. This node is built on two levels: the lower one to connect the rods; the upper one to connect the vertices of panels. The two groups of structural elements can be slightly spaced without inducing any geometrical distortion on the node, and with the advantage of presenting only the glass surface on the outside of the shell to benefit from a continuous reflectivity and water-tightness.

The valence 3 node has fostered a compact and aesthetically pleasant design in spite of the demand of stiffness, strength, dry-assembly moving spaces that on the other hand are more easy to accomplish with an oversized component.

Like TVT nodes, the glass to steel contact is avoided by the interposition of softer material such as aluminium type EN AW–6060 T5 and polyethylene. Moreover, these spacers have to consider the tolerances of panels and to guarantee the contact of steel and glass at the assembly phase. The tolerance of glass panels is the weakest point in the system and is related with the outline precision and in turn with the accuracy of bending and lamination. This tolerance should be within the limit of ± 3 mm (Bundesverband Flachglas 2011), but also higher values of ± 5 mm have been experimentally found (Bukieda et al. 2018). The control of bending geometry constitutes the major issue. It is recommended to realize prototypes to be surveyed and tested with real load scenarios. If larger tolerances are found on the prototypes, then the node design has to be updated in order to include additional adjustment capability, to embed thicker spacer material or to increase the clamping area. These scenarios affect the structural behavior of the connection, which is to be tested and better characterized in order to update the FE model.

The current node has been verified for robustness, namely to be over resistant with respect to the forces transferred from the incident elements. Moreover, the feasibility of all the assembly movement have been checked since one of the strengths of this system is the dry assembly, which favors an easy construction and replacement of damaged components.

3 Case study description, analysis method and materials

3.1 Geometry of the SGS

In terms of geometry, the present case study is obtained from a sphere with 6 m-diameter. This surface is segmented with a regular tessellation producing the truncated icosahedron, which is an Archimedean solid, one of 13 convex isogonal nonprismatic solids whose faces are two or more types of regular polygons. In this case, there are 12 all-equal regular pentagonal faces, 20 all-equal regular hexagonal faces (Pottmann 2007). Regular polygons are equlateral and equiangular.

The geometrical approach to generate the truncated icosahedron is the typical tessellation sequence that starts from the icosahedron solid and cut each vertex by

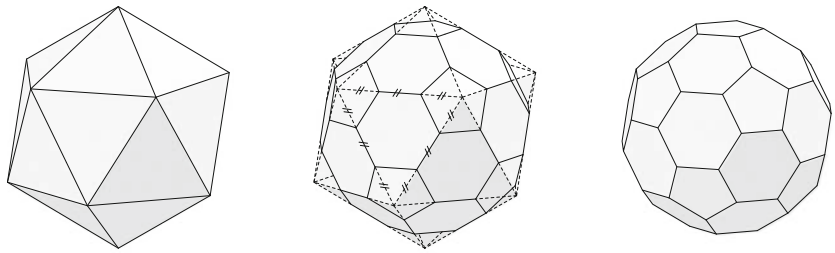

Fig. 5 Geometric construction of the truncated icosahedron from the icosahedron

Table 1 Metrics of the suspended sphere case study

	Unit	Value
Area	m^2	106.30
Volume	m^3	97.95
Diameter	mm	6000
Mesh edge length	mm	1210
Num. edges		90
Num. pentagon faces		12
Num. hexagonal faces		20
Num. nodes		60
Node valence		3

Area and Volume are referred to the truncated icosahedron as per Eq. 1

means of a plane, whose normal is equal to the vertex normal (Fig. 5). Two possible solids can be derived: the truncated icosahedron with constant face area and the truncated icosahedron with constant edge length. This latter strategy has been selected and, in particular, the planes divide the original icosahedron edges in three segments. Some of the main quantitative information such as area A and volume V can be evaluate analytically from the edge length l (Eq. 1). The main measures of the case study are included in Table 2.

$$A = \left(30\sqrt{3} + 3\sqrt{25 + 10\sqrt{5}}\right) l^2 \quad ;$$
$$V = \frac{1}{4}\left(125 + 43\sqrt{5}\right) l^3 \qquad (1)$$

The truncated icosahedron has 60 all-equal vertices of valence 3. After the truncation the nodes valence goes from 6 to 3 with a beneficial effect on the design of connections for low valence nodes (Table 1).

The vertices and the edges of the truncated icosahedron are selected as nodes and as unbonded reinforcement of the structure respectively. The panels of the structure are obtained by projection of the faces on the sphere that pass through the vertices of the solid. Thus, both the reinforcement and the panel vertices merge in the same set of nodes. The faces of the structure are double curved spherical panels of 3 m radius, their main dimensions are included in Table 2 and illustrated in Fig. 6. All panels have rounded vertices of radius 100 mm.

The structure is supported by a suspension system made of 5 masts and a net of cables, which emphasizes the weightless appearance of the sphere, which has a mass $m = 6600$ kg. The cables are fastened to 10 nodes of the sphere, of which 5 belong to the lower pentagon of the structure. These lower-pentagon nodes are not directly attached to the cables but are sustained by a pentagonal steel ring. From the dynamic point of view, this support system constitutes a decoupling of the sphere motions from the foundation, which could result useful to decrease the demands for earthquake or wind excitation. A rendered view of the SGS is in Fig. 7.

Table 2 Geometry of the two types of panels

	Area (m^2)	Circumscribed circle radius (mm)	Rise (mm)	Vertex angle (deg)
Pentagon	2.69	2060	165	108
Hexagon	4.12	2421	255	120

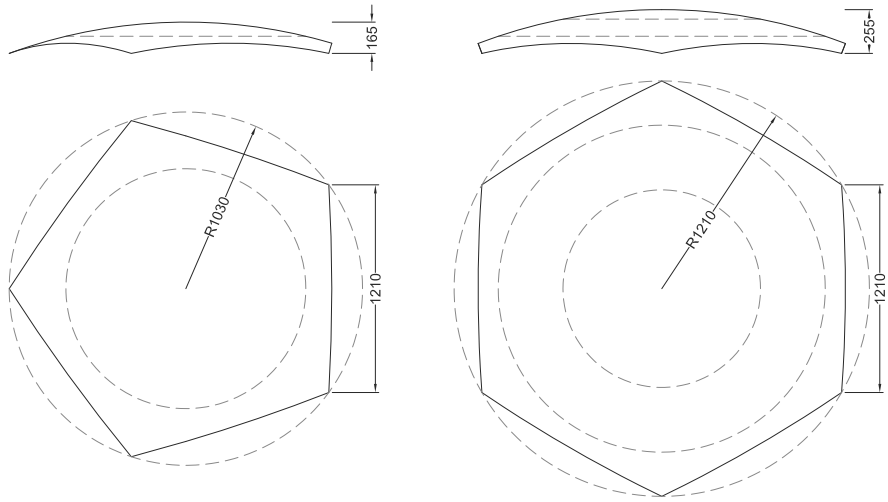

Fig. 6 Geometry of the regular pentagonal and hexagonal panels used in the SGS

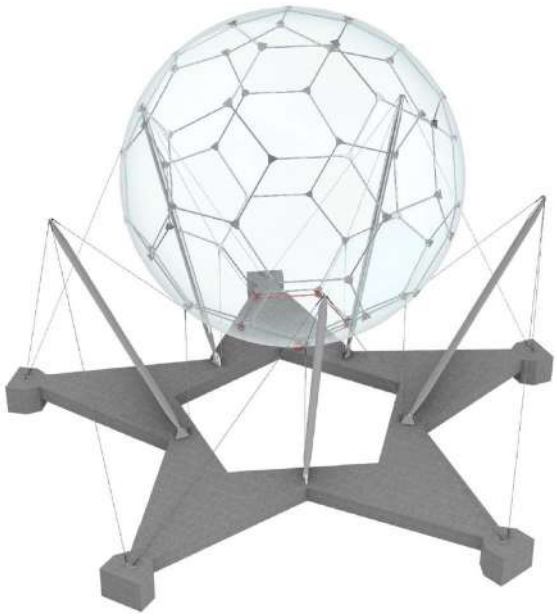

Fig. 7 Impression of the SGS case study in a urban environment

3.2 Analyses

The validation of the proposed concept is tackled at two levels of investigation: local and global level. The local level analyses regard the structural response of regular pentagonal and hexagonal panels in terms of stress, displacement and buckling. An additional outcome is the calibration of a reduced truss model to be used for design purposes in the global level analyses. This latter regards the static response of the whole structure and the robustness evaluation in the 'worst case scenario' (WCS). Then, a full detailed model is built and all load combinations are explored.

Depending on the conceptual design and on the employed joints, the panels are expected to perform a rocking dynamic motion within their polygonal frame. This effect is neglected in the present case study as it goes beyond the objectives of the work. However, a dynamic model has been created to study the natural frequencies of the system. In this model, the whole sphere is considered as rigid system.

The following sections are organized to include models and results for each level of investigation. Although they are based on the SGS geometry, local analyses in Sect. 4 and global analyses in Sect. 5 present approaches and results that can be extended to other case studies based on the present concept. Instead, the content of Sect. 6 pertains the suspended systems which are not necessarily related to glass shells.

All FE models are realized by means of a commercial software (G+D Computing 2005, 2010).

3.3 Materials

Glass and common structural steel are the two materials considered in the simulations. The glass panel is made of two plies of 10 mm glass, which are gravity bent, chemically strengthened and laminated with interposed a 1.52 mm PVB layer. Detailed specifications are included in Table 3. All the materials have been defined as isotropic linear elastic.

Table 3 Components and material adopted for the FE models

Component	Material	Type	Size/cross section	Mech. Parameters
Glass panels	Bent, laminated	CS	$10 + 1.52 + 10$ mm	$E_g = 70$ GPa; $\nu = 0.23$
Reinforcement rods	Structural steel	S275	$D = 33.7$ mm; $s = 3.2$ mm	
Pentagonal ring	Structural steel	S275	$D = 76.1$ mm; $s = 5.0$ mm	$E_s = 210$ GPa; $\nu = 0.3$
Masts	Structural steel	S275	$D = 168.3$ mm; $s = 10$ mm	
Cables	Steel		$D_{eq} = 18$ mm	$E_c = 200$ GPa; $\nu = 0.3$

CS stands for chemically strengthened

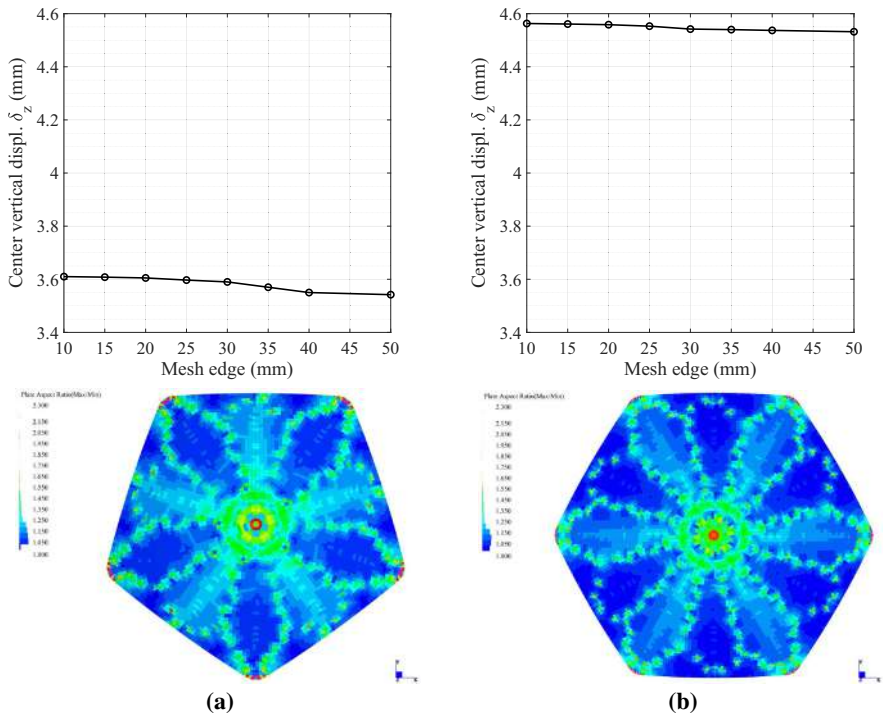

Fig. 8 Sensitivity analysis of FE plate model of the bent glass panels at the top and aspect ratio contour map of the 20 mm-edge-size mesh: **a** pentagon, **b** hexagon

4 Structural response of polygonal doubly-curved glass panels and reduced model calibration

4.1 Model

The bent glass panel has been modeled as FE plate shell elements with an edge size dimension of 20 mm (Fig. 8). For this single-ply model, the equivalent thicknesses of glass have been used. The calibration of the boundary condition is the most demanding part of the work. In the absence of experimental data, the stiffness of the compression-only contact elements is deduced as done for the TVT connections on the basis of the spacer material.

Geometrical and contact nonlinearities are considered in the analysis. The following calculations are preformed in the worst condition for geometry and load within the SGS. In particular, there are three extreme representative loading conditions for both panels: (a) the panel is in a concave position, i.e. at the top of the structure, with gravitational load and snow; (b) the panel is in a convex position, i.e. at the bottom of the structure, with gravitational load; (c) the panel that has one or more vertices on the supports, in this case an asymmetrical reaction force is to be summed to face

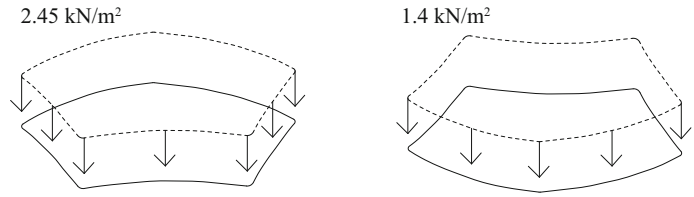

Fig. 9 Geometry and loads on panels: **a** convex, **b** concave position

loading. Among the three, the case (a) is the better performing and the case (b) is the worst condition (Fig. 9), therefore case (c) is omitted for sake of brevity.

4.2 Stress and displacement results

The results of conditions (a) and (b) are shown in Fig. 10, from which it is possible to show how different is the behavior of the panels in both cases due to the shape effect. While in the convex position tensile stress is almost null, in the concave position it reaches the value of $\sigma_{11} = 29.4$ MPa because the panel behave as a tensile membrane.

For the deformations, the support nonlinearity is decisive. The convex panel is well supported by the compression-only support and then result very stiff. On the other hand, the concave panel suffers from a less stiff clamping reactions. This effect appear even more enhanced considering that the SLS load on the concave panel is about half of that on the convex one. However, even considering the limitation of CNR (2012)

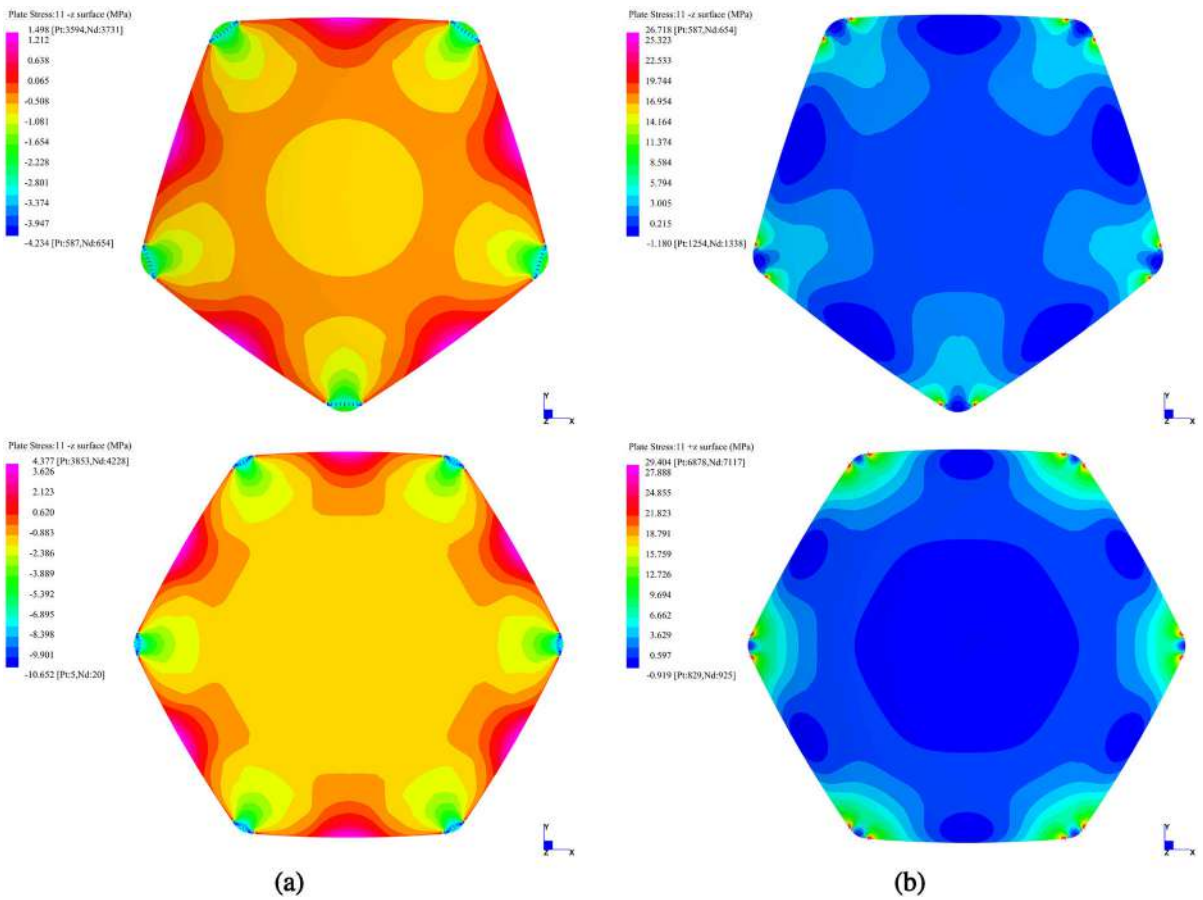

Fig. 10 Maximum principal stress results for panels in **a** convex, **b** concave position

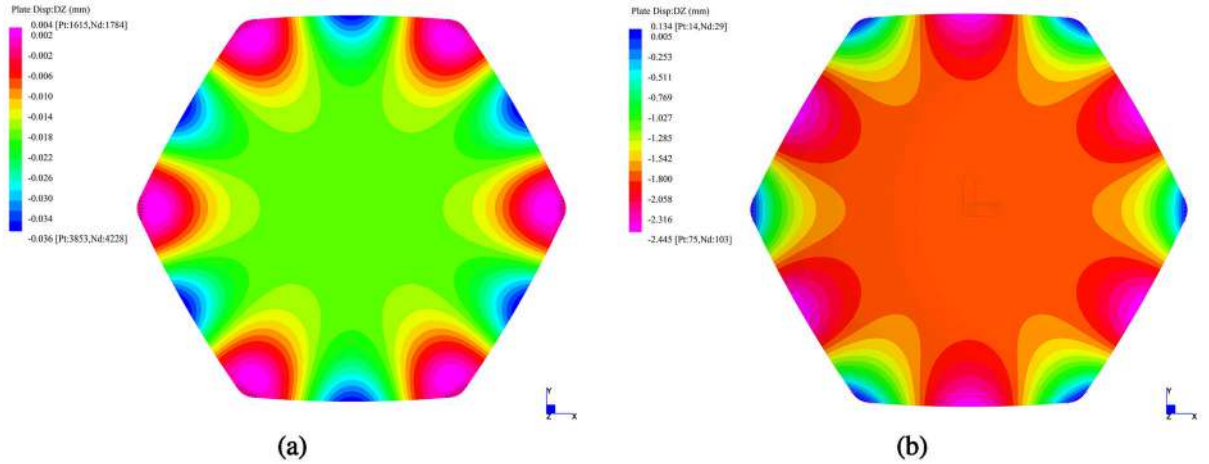

Fig. 11 Deformation for the hexagonal panels in **a** convex, **b** concave position

$i/100 = 12.1$ mm the maximum deflection of the convex panels results well within this limit.

4.3 Buckling

For compressed panels, a risk to prevent is to have a buckling failure for design loads. Although extensive literature has been developed on glass buckling (Bedon and Amadio 2014; Bedon et al. 2015; López-Aenlle et al. 2016; Bedon and Amadio 2016; Luible and Schärer 2016; Liu et al. 2017; D'Ambrosio and Galuppi 2020) including cold bent glass performances (Galuppi et al. 2014), heat curved panels seems to be not investigated. Due to the impossibility to rely on realistic methods, a first attempt can be to look at analytical solutions and make safe assumptions (Fig. 11).

To be on the safe side, the buckling analysis could be performed at the layered limit, so on a single ply of the panel, neglecting the contribution of the interlayer and the collaboration with the twin panel. A closed form solution of the buckling load (Timoshenko and Gere 2012) for shallow spherical cap shell with pin supports and a uniformly distributed pressure is given in Eq. 2.

$$q_{cr} = \frac{2E}{\sqrt{3(1-\nu^2)}} \left(\frac{t}{R}\right)^2 \tag{2}$$

The values of $t = 10$ mm and $R = 3$ m are adopted. However, neither the boundary conditions nor the result is satisfying because in the first case, the actual panel is point supported, and in the second case, an upper bound for the solution was expected but the equation led to a value of $q_{cr} = 930$ kN/m^2 that equals to a load multiplier of 379.6, namely number of times the design pressure on the concave panel 2.45 kN/m^2. This results is too high to be regarded as plausible.

The FEM linear buckling analysis led to a more realistic yet still very high value of the buckling factor $\lambda = 12.53$, taking as initial condition the load on the convex hexagonal panel. Realistic boundary conditions are included.

Again, the obtained value is not physically plausible because if the panel is loaded by the critical buckling load using a static solver it can be observed that the maximum principal stress is far beyond the characteristic strength of the material. It means that the panel tensile failure occurs before buckling. From an incremental nonlinear analysis of the panel, the characteristic strength is reached for a load multiplier of 3.15. Also in the case of asymmetrical loading conditions, glass tensile failure remains the most likely failure modality; these scenarios need to be checked via incremental nonlinear analysis.

Further investigations are needed to confirm these preliminary results and most importantly to include the panel imperfections that are to date unknown and have been neglected.

4.4 Stiffness-based reduced model calibration

One of the main advantages of using a point-supported panel as single structural unit is that it can be reduced into an assembly trusses, whose elements are incident

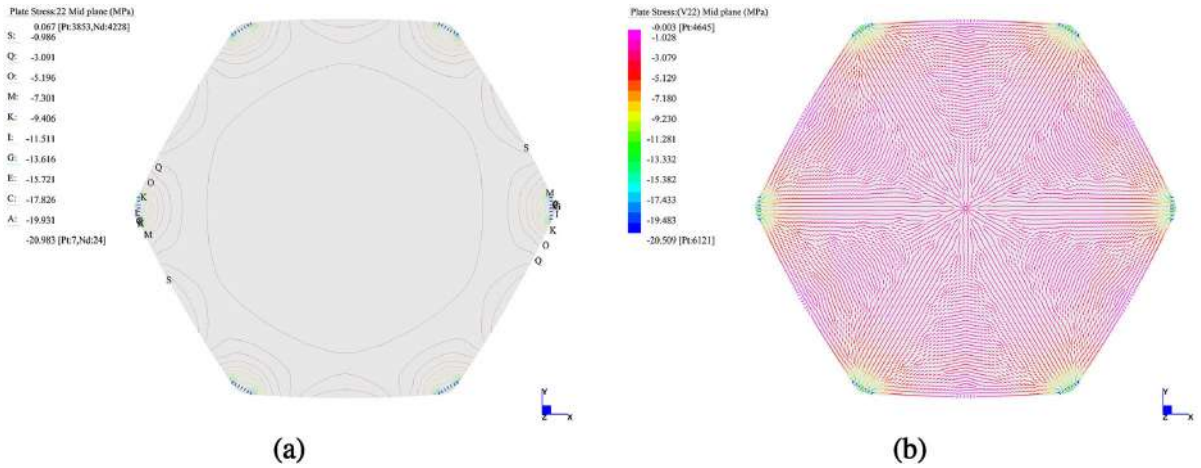

Fig. 12 Minimum principal stress on the hexagonal panel: **a** isolines; **b** vector field

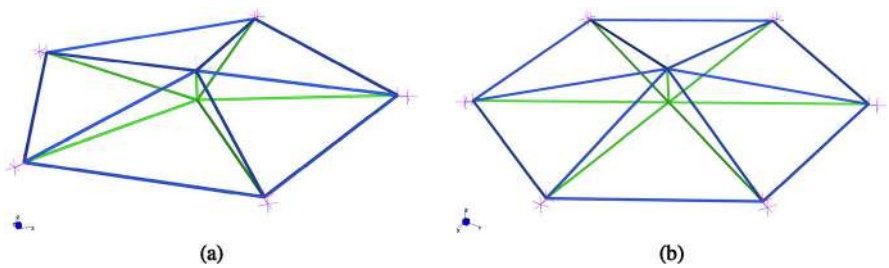

Fig. 13 Stiffness-based reduced truss model for **a** the pentagon and **b** the hexagonal panel

Table 4 Adopted cross section in the glass panels' reduced model

Component	FE type	Material	Cross section/stiffness	Mech. Parameters
Hexagon blue edges	Truss	Glass	Round $D = 15.3$ mm	$E_g = 70$ GPa; $\nu = 0.23$
Pentagon blue edges	Truss	Glass	Round $D = 15.2$ mm	$E_g = 70$ GPa; $\nu = 0.23$
Green edges	truss	Glass	Round $D = 13.0$ mm	$E_g = 70$ GPa; $\nu = 0.23$
Link to the main node	point contact	–	$k = 560$ kN/m	(Compression only)

Reference to colors of Fig. 13

into the support nodes. This is justified by the resulting stress paths on the shell element (Fig. 12). In other works concerning polygonal tessellations such as Froli and Laccone (2017), a fan-shaped truss grid has been used to simulate the stiffness contribution of plexiglass panels that infill Voronoi meshes.

For the present structural concept, a simply fan-shaped truss with the central node located on the panel center would have been very sensitive to support conditions and non-membrane loading, and so not representative of the actual behavior. Therefore, it is added to a second flat layer of truss (i.e. in this case this is equal to a projection on the flat face) and ring elements. Thus, a volumetric tetrahedral structure is formed, and the shape stiffness given by double curvature is suitably modeled. The model is represented in Fig. 13 while the geometric and mechanical properties adopted are included in Table 4.

A comparison based on the stiffness of the two models (the plate and the reduced truss) is used to calibrate the size of the truss elements. A stress criteria has indeed no meaning since stress verification can be executed on more accurate plate models. The springs at the vertices are equivalent to the nonlinear supports

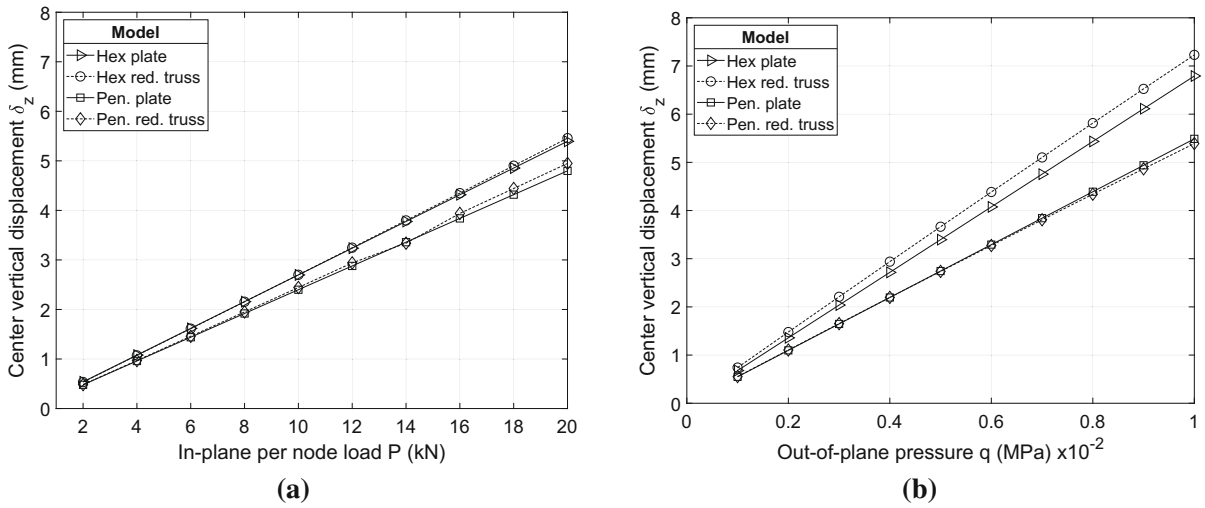

Fig. 14 Stiffness calibration of the reduced models: **a** in-plane load; **b** out-of-plane load

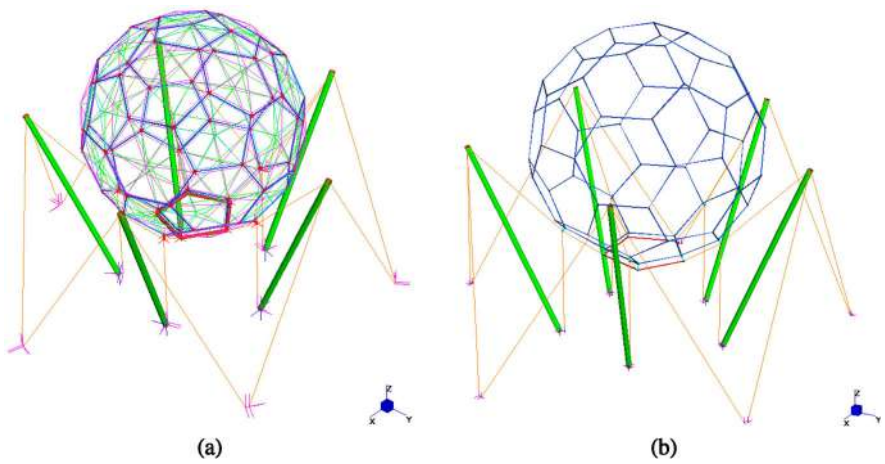

Fig. 15 Global models: **a** full model with reduced truss as glass panels; **b** worst-case scenario model

of the plate model. The calibration has been executed for both in-plane and out-of-plane loading. In the first case, the vertices are loaded with forces that are within the range of the expected reactions at the supports. In the second case, the truss is loaded with vertical loading equivalent that are equal to the total face pressure divided in proportion to the Voronoi area of the mesh (Fig. 14).

The reduced model is employed into the design of the truss and the estimation of the WCS performance of the structure.

5 Global analyses

5.1 Model

In a first stage, a global model of the SGS is built (Fig. 15) in order to design the steel components. A reduced model as per Sect. 4.4 is employed to describe the stiffness of bent glass panels. Beam elements are used for the rods and for the masts, cut-off bar elements are used for the cables. Cross sections and material as per Table 3 are used. Nonlinear spring dampers simulates the connection of the panels vertices with the steel nodes.

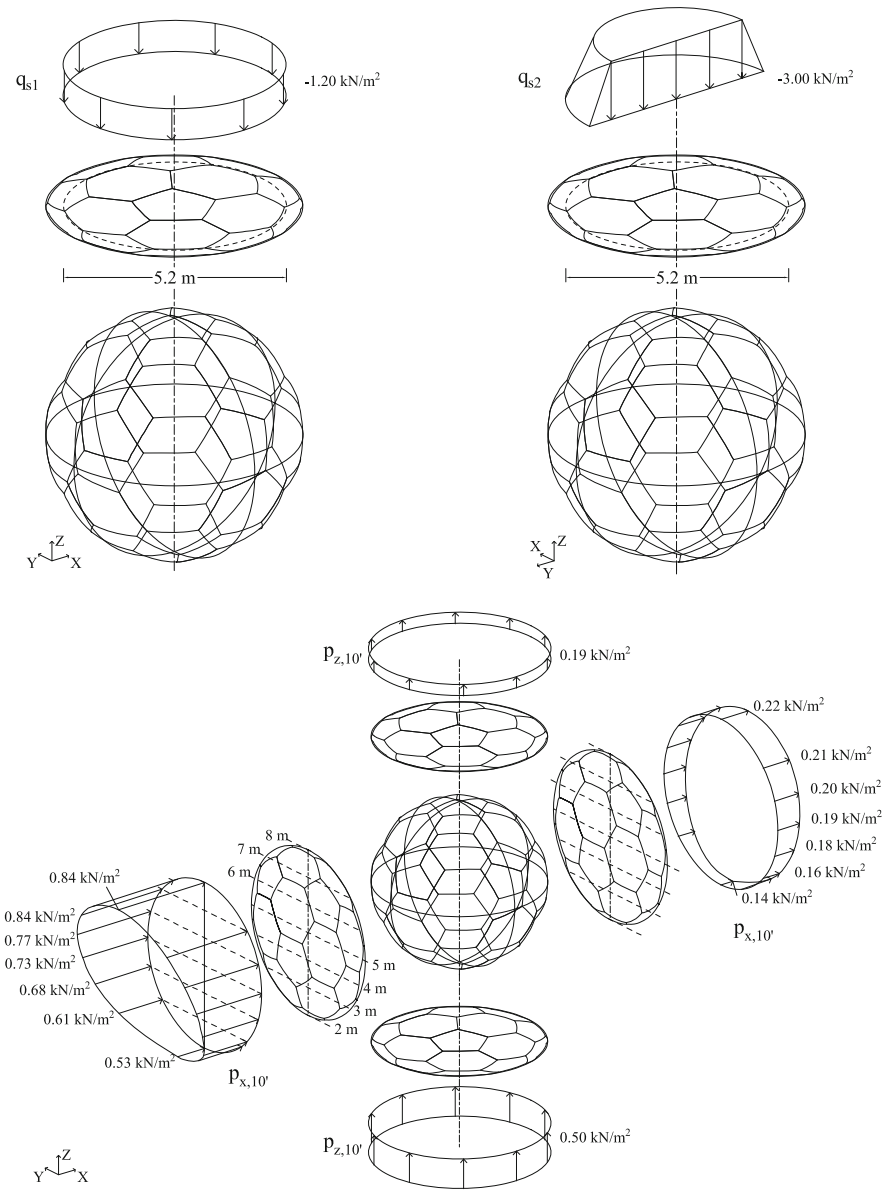

Fig. 16 Model and loads on the global model: at the top left, symmetric snow load $Q_{snow,sym}$; at the top right asymmetric snow load $Q_{snow,asym}$; at the bottom 10' wind load $W_{10'}$

The loads are applied on the vertices of the truss that represent the panels in proportion to the Voronoi area. Geometrical and contact nonlinearities are considered in the analysis, while materials are assumed linear. In this phase, gravitational and wind loading in X direction ($W_{x,3''}$) are used. Their intensity and geometry is later specified (Figs. 16, 17).

In order to make comparisons with the ULS, another model named WCS has been realized to simulate the 'worst case scenario'. In this model, the panels are supposed to be cracked and unable to play any structural role, except to transfer loads on the steel nodes. Therefore, they are removed and their load is directly positioned on the nodes.

With the aim of testing the response of the structure with respect of all kind of loads, a full detailed model is developed. This model includes the panels as FE plate elements with equivalent thickness. The applied loads are schematically represented in Figs. 16, 17 and are combined according to the scheme of Table 5. Since the SLS is governed by the suspension system the SLS combinations are omitted. This model is used to

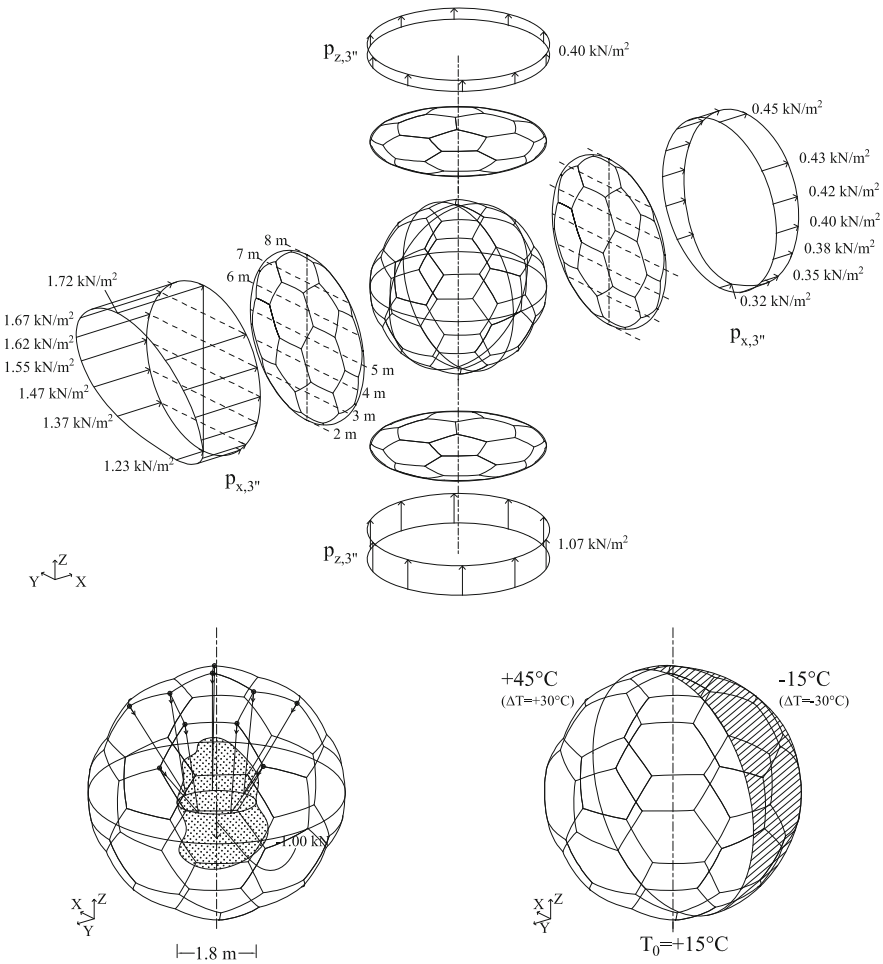

Fig. 17 Model and loads on the global model: at the top, $3''$ peak wind load $W_{3''}$; at the bottom left, art installation load $G_{2,art}$; at bottom right, temperature load $Temp$

Table 5 Coefficients for ULS load combinations employed for the structural verification of the full detailed model (ref. Sect. 5.4)

Name	G_1	P	$G_{2,art}$	$Q_{snow,sym}$	$Q_{snow,asym}$	$W_{x,10'}$	$W_{z,10'}$	$W_{x,3''}$	$W_{z,3''}$	$Q_{k,H}$	$Temp$
ULS1	1.3	1.0	1.5	1.5	0	0.9	0	0	0	0	0.9
ULS2	1.3	1.0	1.5	0	1.5	0.9	0	0	0	0	0.9
ULS3	1.3	1.0	1.5	0	1.5	0	0.9	0	0	0	0.9
ULS4	1.3	1.0	1.5	0.75	0	1.5	0	0	0	0	0.9
ULS5	1.0	1.0	0	0	0	0	1.5	0	0	0	0.9
ULS6	1.3	1.0	1.5	0	0	0	0	1.5	0	0	0.9
ULS7	1.0	1.0	0	0	0	0	0	0	1.5	0	0.9
ULS8	1.3	1.0	1.5	0.75	0	0.9	0	0	0	0	1.5
ULS9	1.3	1.0	1.5	0.75	0	0.9	0	0	0	1.5	0.9

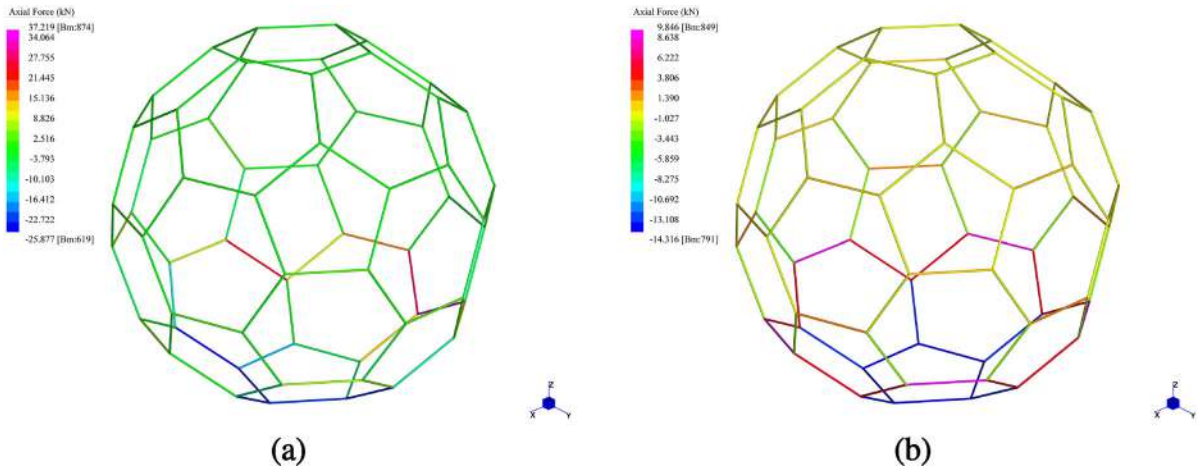

Fig. 18 Axial forces on the rods at the ULS for the model of Fig. 15a: **a** gravity loadings; **b** prevalent 3″ X wind combination (glass elements included by means of reduced models and suspension system are hidden for output display reasons)

make comparison with a similar state-of-the-art structure with glued butt joints.

5.2 Stress and displacement results

As demonstrated also in the previous Sect. 4, using a target geometry of a sphere this case study has the advantage of highlight simultaneously different local behavior of the components. An illustrative output is in Fig. 18, in which are shown the axial forces on the rods. Glass panels and the suspension system are hidden for output reasons. It can be deducted that for gravity loading (Fig. 18a) the upper cap of the sphere is mostly compressed with small values of axial force, showing that glass is working in the best condition and carries most of the shell action. On the lower side, the panel is in convex position and its stiffness is lower, and as demonstrated by axial forces the steel becomes the stiffer component.

Same discussion can be made for the wind load combination shown in Fig. 18b: rods in the wind direction are compressed, the upper cap is still behaving as a shell, while on the other side maximum absolute values of axial forces occur on the rods.

As expected, the maximum deformation achieved at the SLS is also a function of the deformation of the supports. This dependency is discussed in Sect. 6, however it is possible to quantify the stiffness of the structure by comparing the displacement at the SLS in the present model (Eq. 3a) with that of the model used in the next paragraph to measure the redundancy subject to the same SLS load (Eq. 3b). Within the framework of the same geometry, support and loading conditions, this can be regarded as comparison of a structural shell designed in accordance with the proposed concept and a grid shell. It provides a measure of the contribution of glass as structural material.

$$\delta_z = 11.0\,mm \leq D/500 = 12\,mm$$
$$\delta_x = 32.7\,mm \leq D/180 = 33\,mm \tag{3a}$$
$$\delta_{z,WCS} = 33.0\,mm$$
$$\delta_{x,WCS} = 66\,mm \tag{3b}$$

5.3 Redundancy

An effective measure to quantify the redundancy is derived by comparing the safety factors achieved by the steel components in the two models under gravity loading: full model at the ULS (Fig. 18a) and WCS model (Fig. 19). Table 6 shows the safety factors of the most stressed steel elements in both cases. Because the SGS manifests either membrane and bending forces, the rods are stressed by all forces, therefore they should be consequently considered in the verification.

The safety factor SF in the WCS model is as expected lower with respect to that in the ULS. In the WCS, glass is in a fractured condition, so it provides no stiffness contribution but it is still able to distribute load to the rods. Therefore, the deformability of the struc-

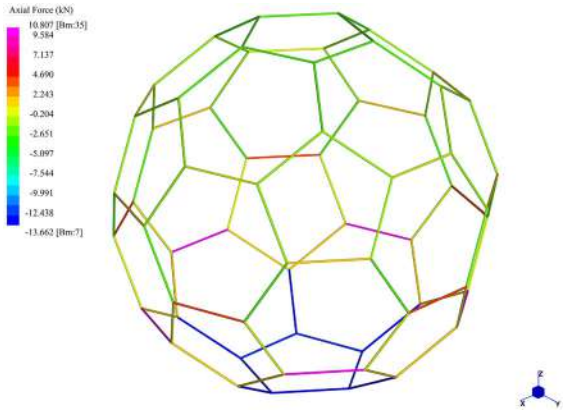

Fig. 19 Axial forces on the WCS model at the ULS for the model of Fig. 15b (loads are applied at the nodes since the glass has no load-bearing function)

Table 6 Safety factor SF on steel rods and redundancy R evaluation

Load case	SF_i	$SF_{WCS,i}$	$SF_i/SF_{WCS,i} = R$
ULS	2.94	1.02	2.88

ture increases with a consequent increase of bending moments on the rods. The almost-unitary value of the SF_{WCS} reveals that the structure is still able to bear the dead load without collapsing, and allows the operators to remove the causes of failure and to replace the components.

From the ratio of the two safety factors, a redundancy factor R of about 3 is derived, and it can be considered a good result despite the mechanical complexity of this case study. The value 3 bound has been assumed in similar work (Weller et al. 2008; Laccone 2019).

As a matter of fact, the rods are well sized and perform the double function of reinforcement, as demonstrated in asymmetric loading conditions (shown in Fig. 18b), and of robust skeleton to avoid collapse in extreme scenarios.

5.4 Detailed model and comparison with an all-glass structure with glued butt joints

The ULS performances of the SGS are quantified through a full detailed model that includes the glass panels as FE plate elements (Fig. 20a). The output confirms the statics of the present structural concept: in particular glass is mainly working as a compressed membrane; the rods keep the joints in their position and sustain tension load when the edge is tensioned, since glass panels have compression-only constraints and can escape relevant tension stress. However, maximum principal stress occurs in the nodes' closeness but it results within the material capacity. Although the lower part of the sphere is less efficient because distributed loads stress glass as a tensioned membrane, a good safety level is maintained due to the grid of rods.

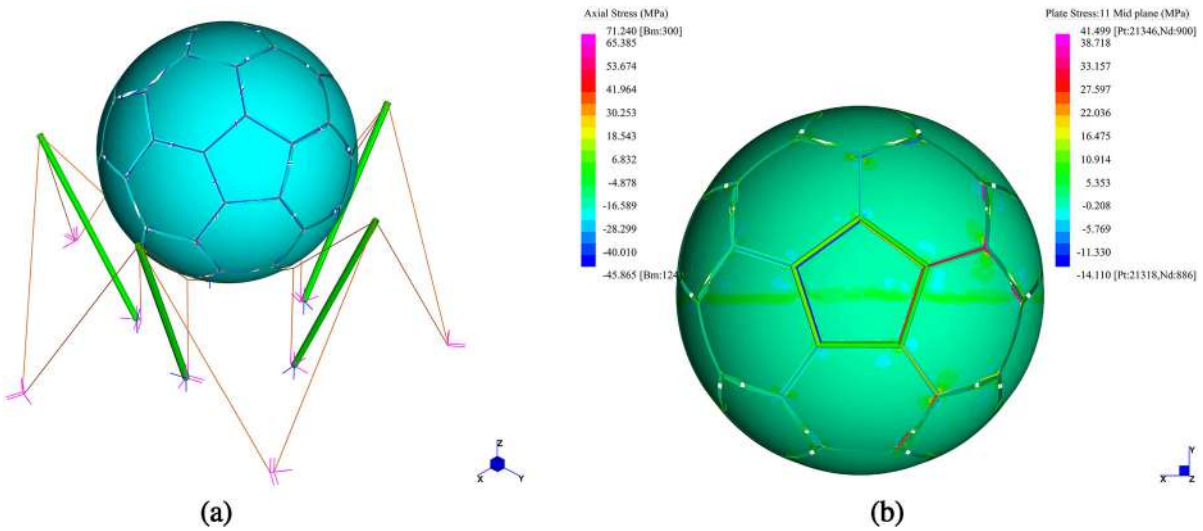

Fig. 20 Full detailed model: **a** model; **b** ULS4 results (bottom view, the suspension system is hidden for output display reasons)

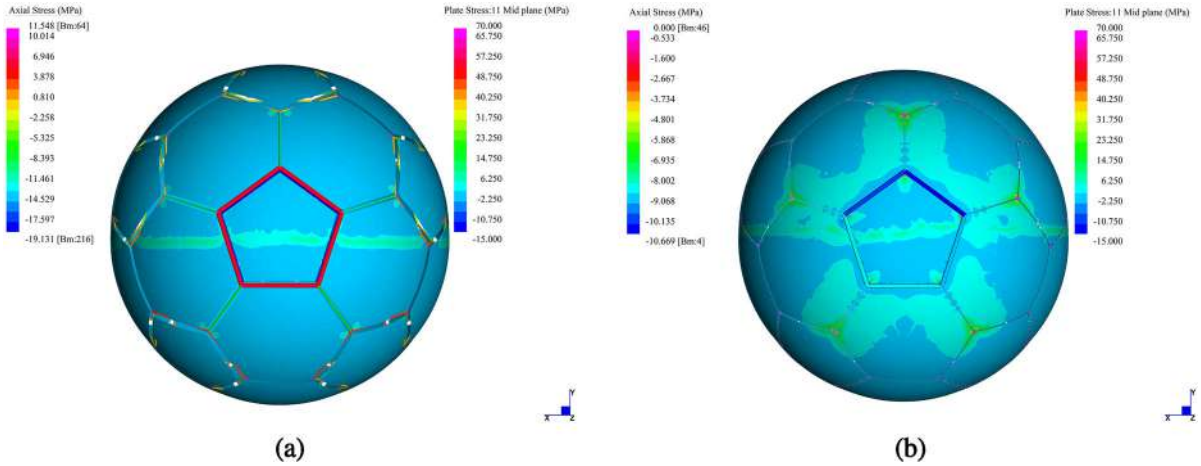

Fig. 21 Comparison of the present concept **a** with an all-glass concept with glued butt joints **b** for the SGS geometry: results for the ULS1, $G_{2,art}$ has not been included in the analyses (bottom view, the suspension system is hidden for output display reasons)

In general, these effects can be observed for all load cases.

An exception is the temperature load. Since no detailed environmental studies are used, it is supposed to have a variation of $\Delta T = \pm 30°$ on two halves of the surface (see as ref. Fig. 17). This loading geometry is conventional and it is established to maximize the stress and deformation within the loads combination. The most remarkable effect of temperature occurs on the 'cold' side of the sphere. Hence, the glass shrinkage, which is lower that the steel, imposes a deformation on the steel rods that force them to stretch. This effect is mitigated by the spacers at the joints. The reverse effect on the 'warm' side does not take place due to the compression-only glass support. Lastly, the stress induced on the panel at the transition of shadow zone results within the material capacity.

The static response of this model is compared with a similar state-of-the-art concept, which is an all-glass shell with glued butt joints. This model apopts the same panels' geometry and a constant 10 mm width joint as in Blandini's prototype (2005) along all edges of glass panels. The adhesive with Young's modulus of $E_{adh} = 1\ GPa$ is simulated with linear springs, whose properties are deduced from the work of Bagger (2010) (FacC_adh1 model). There are no rods in the model, except for the lower pentagonal ring. It constitutes the support of the sphere and sustains tension load. To avoid introducing punctual loads, the $G_{2,art}$ load case is not included. A comparison for the snow-prevailing load combination is reported in Fig. 21. The figure reports the elements of the bottom hemisphere and it shows that the steel rods relieve glass from carrying tensile forces, which instead using the state-of-the art concept are sustained more diffusely by glass. On the top hemisphere, similarly in both cases, glass is mainly compressed. The adoption of a steel grid has an important practical outcome since it avoids the use of rigid scaffolding for the panels lying, which is instead necessary for the realization and curing of glued butt joints.

6 Influence of the suspension system

Based on the SLS results obtained from the global model in Sect. 5, it appears evident that the maximum horizontal and vertical displacements of the structure are related to the stiffness of the suspension system. Only a minimal part of the global displacement are due to the deformation of the sphere. A major role is played by the post-tensioning force of the cables. Figure 22 shows parametric plots of the maximum vertical and lateral displacement of the structure with respect to the applied post-tensioning force. It is evidenced that good deformation parameters can be obtained by adopting a value of 45 kN.

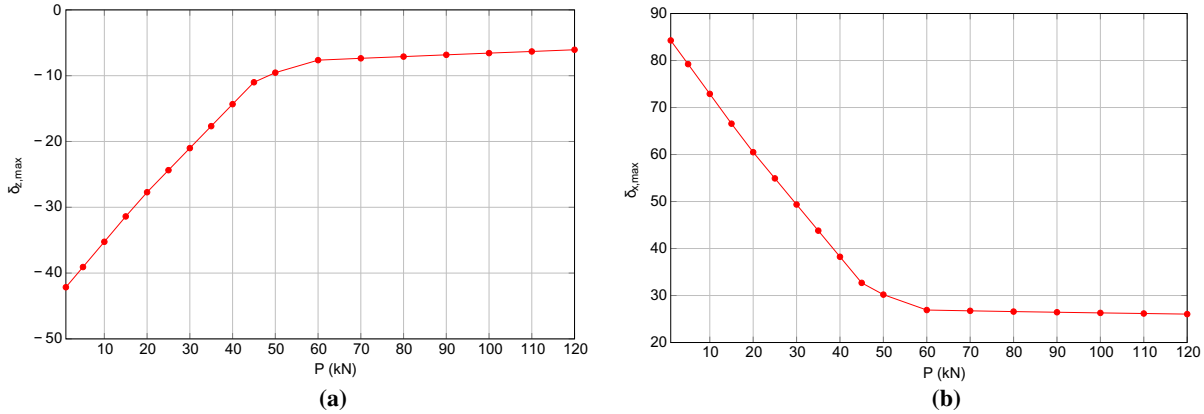

Fig. 22 Parametric plots of the influence of the cable post-tensioning P on the maximum displacement of the SGS (a) $\delta_{z,max}$ in the vertical and (b) $\delta_{x,max}$ in the horizontal direction

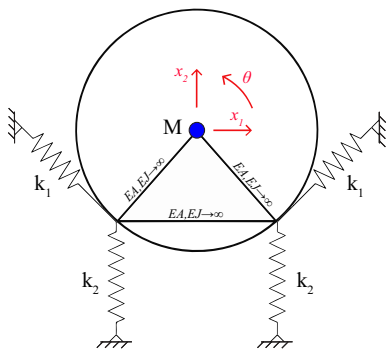

Fig. 23 Schematic graphic representation of the 2D analytical dynamic model

6.1 Modal analysis and parametric investigation on the suspended system

An additional aspect related to the suspension system concerns the dependency of natural frequencies of the SGS on the post-tensioning. In order to generate these parametric plots, first a FEM 2D and then a 3D model have been created.

The 2D model exploits one of the symmetry axis and represent cumulative inertial components (mass $M = 6600$ kg, rotational inertia $I = 297$ kg/m^2) and equivalent stiffness of the cables, which have been projected on the symmetry plane. The SGS is considered as a rigid body. As a 2D plane model, it has three Lagrangian parameters. To check the FEM model a simple analytical model has been developed (Fig. 23) from the dynamic equilibrium (Eq. 4).

$$[M]\{\ddot{x}\} + [K]\{x\} = \{0\} \tag{4}$$

The eigenvalues of the system in Eq. 5 provide the natural frequency of the non-post-tensioned system (Eq. 6).

$$\begin{cases} M\ddot{x_1} + \left(k_1\sqrt{2}/2 + k_1\sqrt{2}/2\right) x_1 = 0 \\ M\ddot{x_2} + \left(k_1\sqrt{2}/2 + k_1\sqrt{2}/2\right) x_2 + (k_2 + k_2)x_2 = 0 \\ \frac{1}{2}Mr^2\ddot{\theta} + (k_1 r + k_1 r)\theta + \left(k_1\frac{l}{2} + k_1\frac{l}{2}\right)\theta = 0 \end{cases} \tag{5}$$

$$\begin{cases} f_1 = 8.35\ Hz \\ f_2 = 12.22\ Hz \\ f_3 = 16.07\ Hz \end{cases} \tag{6}$$

However this model is affected by an error of having neglected the post-tensioning induced by the weight of the structure, which will be considered in the FEM model. Building on the 2D model knowledge, a 3D model has been developed.

6.2 Results of modal analysis

The results of the parametric investigation on the natural frequencies are included in Fig. 24. It can be observed that the post-tensioning force has not a large effect on the natural frequencies. Only providing or not post-tensioning forces constitutes a remarkable modification of the system. The modal analysis on the 3D model (Fig. 25) shows results that are in line with the 2D model and are affected by the same sensitivity.

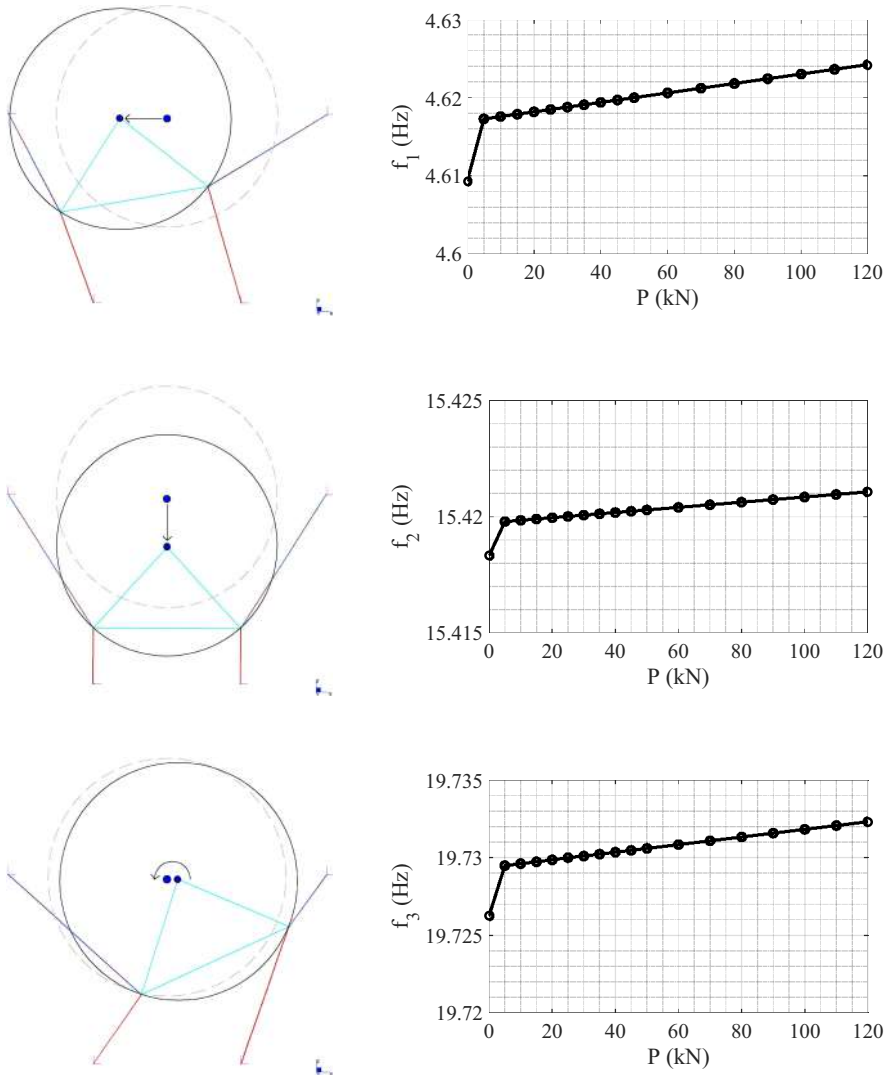

Fig. 24 Parametric investigation on the effect of post-tensioning on natural frequencies using the 2D model

It is possible to conclude that the post-tensioning of the suspended system has to be sized in a static scenario since the dynamic model is only secondary affected by this value. In spite of this little sensitivity, a more important outcome of the modal analysis can be traced: the SGS considered as a rigid body has typical frequencies of an isolated structure. Consequently, in a full dynamic analysis of the SGS, the structural demand is supposed to be filtered and lowered by the suspension system. Moreover, the cables can be equipped with damping devices to add an energy dissipation capability to the system.

7 Conclusions

The proposed structural concept has been applied to the case study of a 6 m-diameter suspended glass sphere (SGS). This structure is a thin shell made of spherical pentagonal and hexagonal panels, coupled with a grid of straight rods. Hence, glass is used as a structural material.

This case study is particularly meaningful because it evidences the strengths of the concept. Indeed, the geometry of the loads and the components within the structure stresses the panels and the rods quite differently. It works best when the panels are concave and

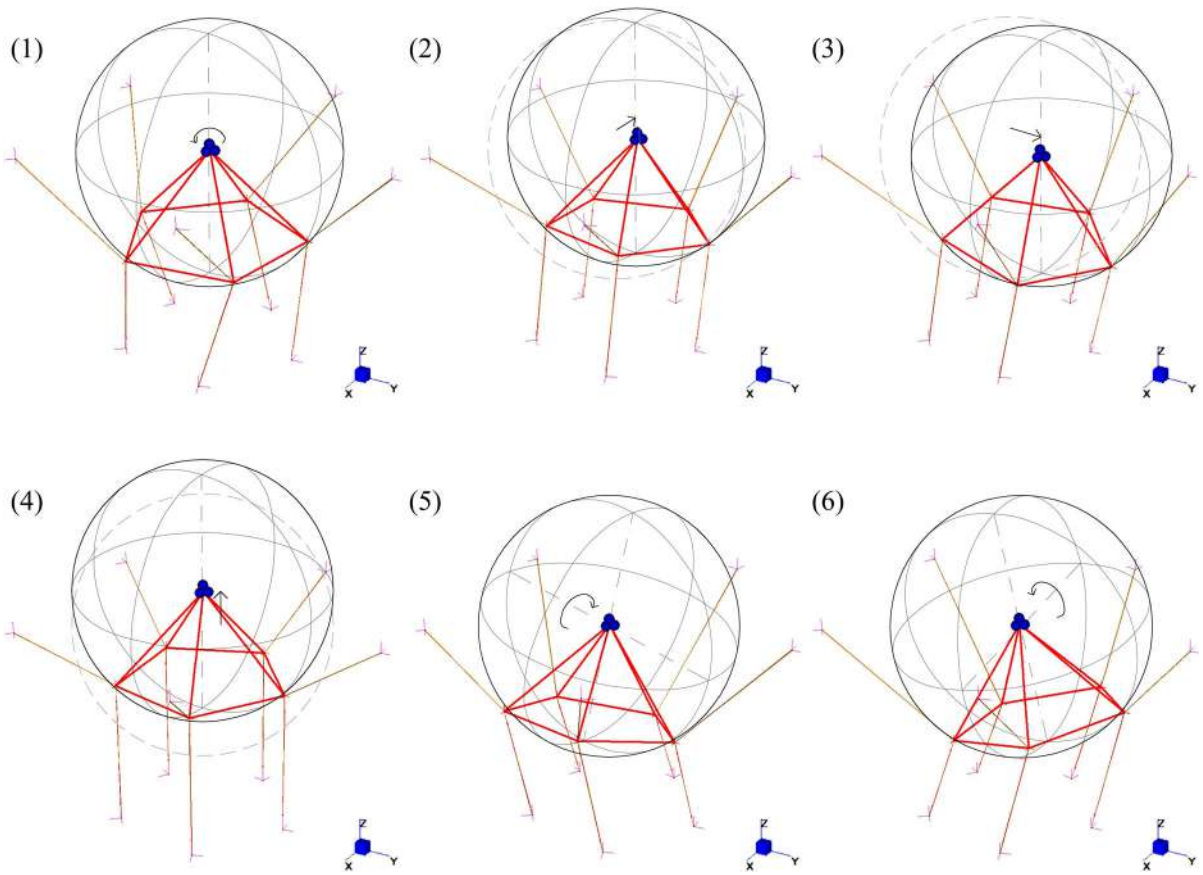

Fig. 25 Modal analysis on the 3D model

well compressed, in this case the structural capacity of glass is exploited and the rods are marginally utilized. So, the concept appears very promising, particularly suited for compressive structures. On the other hand, due to the nonlinear nature of the clamping, loading convex panels stresses more the rods. This feature is useful also in wind suction areas or in case of asymmetrical loads. This makes the concept a valid alternative with respect to the state of the art since the tensile stress on glass lowers and accordingly the risk of cracking.

The redundancy concept envisages the possibility to entrust the whole bearing capacity to the grid of rods in an extreme scenario where the panels are simultaneously cracked and then able only to transfer the load at the nodes. The validation has been performed on a global FE model in which is observed an increase of the bending forces on the rods that lowers the safety factor of the grid. The ratio of the safety factors on the steel components provides a measure of redundancy, which reaches in this case a safe-enough level of about 3.

As an outcome of this holistic approach to the conceptual design that considers architectural and structural requirements, the SGS results feasible and safe. Moreover, there are some open points that deserve further investigation.

The hypothesis of a complete glass collapse is one of the possible and more conservative scenarios, however also partial failure of panels might be considered, and both their global and local effect. The concave shape of the panel has an inherent robustness, and even if cracked it may be supposed that it can develop a membrane effect, which could still preserve the bearing capacity yet with a reduced stiffness.

For a detailed structural design and for applications of the concept to other shapes, considering the imperfection is mandatory either at global and at local level. The node design may be updated if in this latter case

different tolerances are required. When facing detailed design or fabrication, the control of bending geometry will represent the major issue to deal with. It is recommended to realize prototypes to be surveyed and experimental validated. In general, literature on the topic of bent glass has to be developed in order to expand its use in architecture and as structural material. Future investigation is required on several topics such as the imperfection size and shape, the buckling and the post-cracked behavior.

Finally, the dynamics of this structure has to be expanded on two directions: on a concept-related level to consider the dissipation capabilities of the dry-clamped glass panels, which is expected to be similar to the TVT behavior; and at the case-study system level to evaluate the isolation and dissipation capacity of the suspension system.

Acknowledgements The authors express their gratitude to Tommaso Fancelli for his collaboration to this work.

Compliance with ethical standards

Conflict of interest The authors declare that they have no conflict of interest.

References

Adriaenssens, S., Ney, L., Bodarwe, E., Williams, C.: Finding the form of an irregular meshed steel and glass shell based on construction constraints. J. Archit. Eng. **18**(3), 206–213 (2012). https://doi.org/10.1061/(ASCE)AE.1943-5568.0000074

Bagger, A.: Plate shell structures of glass: Studies leading to guidelines for structural design. Ph.D. thesis, Technical University of Denmark (DTU) (2010)

Bedon, C., Amadio, C.: Flexural-torsional buckling: experimental analysis of laminated glass elements. Eng. Struct. **73**, 85–99 (2014). https://doi.org/10.1016/j.engstruct.2014.05.003

Bedon, C., Amadio, C.: Shear glass panels with point-fixed mechanical connections: finite-element numerical investigation and buckling design recommendations. Eng. Struct. **112**, 233–244 (2016). https://doi.org/10.1016/j.engstruct.2016.01.024

Bedon, C., Amadio, C.: Glass facades under seismic events and explosions: a novel distributed-tmd design concept for building protection. Glass Struct. Eng. **3**(2), 257–274 (2018). https://doi.org/10.1007/s40940-018-0058-9

Bedon, C., Belis, J., Amadio, C.: Structural assessment and lateral-torsional buckling design of glass beams restrained by continuous sealant joints. Eng. Struct. **102**, 214–229 (2015). https://doi.org/10.1016/j.engstruct.2015.08.021

Bedon, C., Louter, C.: Finite-element analysis of post-tensioned sg-laminated glass beams with mechanically anchored tendons. Glass Struct. Eng. **1**(1), 39–59 (2016). https://doi.org/10.1007/s40940-016-0020-7

Bedon, C., Zhang, X., Santos, F., Honfi, D., Kozłowski, M., Arrigoni, M., Figuli, L., Lange, D.: Performance of structural glass facades under extreme loads-design methods, existing research, current issues and trends. Constr. Build. Mater. **163**, 921–937 (2018). https://doi.org/10.1016/j.conbuildmat.2017.12.153

Belis, J., Louter, C., Nielsen, J.H., Schneider, J.: Architectural glass. In: Musgraves, J.D., Hu, J., Calvez, L. (eds.) Springer Handbook of Glass, pp. 1781–1819. Springer, Berlin (2019). https://doi.org/10.1007/978-3-319-93728-1_52

Blandini, L.: Structural use of adhesives in glass shells. Ph.D. thesis, Institut für Leichtbau Entwerfen und Konstruieren (ILEK), Universitat Stuttgart (2005)

Blandini, L.: Prototype of a frameless structural glass shell. Struct. Eng. Int. **18**(3), 278–282 (2008). https://doi.org/10.2749/101686608785096586

Bruno, L., Sassone, M., Venuti, F.: Effects of the equivalent geometric nodal imperfections on the stability of single layer grid shells. Eng. Struct. **112**, 184–199 (2016). https://doi.org/10.1016/j.engstruct.2016.01.017

Bukieda, P., Engelmann, M., Weller, B.: Testing procedure and the effect of testing machinery on four-point bending of curved glass. ce/papers **2**(5–6), 311–323 (2018). https://doi.org/10.1002/cepa.933

Bundesverband Flachglas e.V: Guideline on thermally curved glass for building applications—BF-Bulletin 009. Tech. rep. (2011)

Casagrande, L., Bonati, A., Occhiuzzi, A., Caterino, N., Auricchio, F.: Numerical investigation on the seismic dissipation of glazed curtain wall equipped on high-rise buildings. Eng. Struct. **179**, 225–245 (2019). https://doi.org/10.1016/j.engstruct.2018.10.086

CNR: Istruzioni per la progettazione, l'esecuzione e il controllo di costruzioni con elementi strutturali di vetro. Consiglio Nazionale delle Ricerche CNR-DT 210/2012 (2012)

Cupać, J., Martens, K., Nussbaumer, A., Belis, J., Louter, C.: Experimental investigation of multi-span post-tensioned glass beams. Glass Struct. Eng. **2**(1), 3–15 (2017). https://doi.org/10.1007/s40940-017-0038-5

D'Ambrosio, G., Galuppi, L.: Enhanced effective thickness model for buckling of LG beams with different boundary conditions. Glass Struct. Eng. **5**, 205–210 (2020). https://doi.org/10.1007/s40940-019-00116-3

Engelmann, M., Hayek, I.E., Friedreich, O., Weller, B.: Post-breakage performance of a spherical glass shell. In: Proceedings of IASS Annual Symposia, vol. 2017, pp. 1–6. International Association for Shell and Spatial Structures (IASS) (2017)

Engelmann, M., Weller, B.: Post-tensioned glass beams for a 9 m spannglass bridge. Struct. Eng. Int. **26**(2), 103–113 (2016). https://doi.org/10.2749/101686616X14555428759000

Feldmann, M., et al.: Guidance for European Structural Design of Glass Components. Publications Office of the European Union, Brussels (2014)

Feng, Rq, Ge, Jm: Shape optimization method of free-form cable-braced grid shells based on the translational surfaces technique. Int. J. Steel Struct. **13**(3), 435–444 (2013). https://doi.org/10.1007/s13296-013-3004-3

Fildhuth, T., Schieber, R., Oppe, M.: Design and construction with curved glass. ce/papers **2**(5–6), 369–381 (2018). https://doi.org/10.1002/cepa.937

Froli, M., Laccone, F.: Experimental static and dynamic tests on a large-scale free-form voronoi grid shell mock-up in comparison with finite-element method results. Int. J. Adv. Struct. Eng. **9**(3), 293–308 (2017). https://doi.org/10.1007/s40091-017-0166-9

Froli, M., Laccone, F.: Static concept for long-span and high-rise glass structures. J. Archit. Eng. **24**(1), 04017030 (2018). https://doi.org/10.1061/(asce)ae.1943-5568.0000285

Froli, M., Lani, L.: Glass tensegrity trusses. Struct. Eng. Int. **20**(4), 436–441 (2010). https://doi.org/10.2749/101686610793557564

Froli, M., Mamone, V.: A 12 meter long segmented post-tensioned steel-glass beam (TVT Gamma). In: Louter, C., Bos, F., Belis, J., Lebet, J.P. (eds.) Challenging Glass 4 & COST Action TU0905 Final Conference, pp. 243–251. CRC Press, Boca Raton (2014)

Galuppi, L., Massimiani, S., Royer-Carfagni, G.: Buckling phenomena in double curved cold-bent glass. Int. J. Non-Linear Mech. **64**, 70–84 (2014). https://doi.org/10.1016/j.ijnonlinmec.2014.03.015

G+D Computing: Straus7 User's Manual (2005)

G+D Computing: Using Strand7 (Straus7)—Introduction to the Strand7 Finite Element Analysis System (2010)

Haldimann, M., Luible, A., Overend, M.: Structural Use of Glass, vol. 10. Iabse, Zurich (2008)

Hayek, I.E., Engelmann, M., Friedreich, O., Weller, B.: Case study on a spherical glass shell. J. Int. Assoc. Shell Spat. Struct. **59**(2), 105–118 (2018). https://doi.org/10.20898/j.iass.2018.196.874

Laccone, F.: Reinforced and post-tensioned structural glass shells: Concept, morphogenesis and analysis. Ph.D. thesis, University of Pisa (2019). https://doi.org/10.13131/unipi/etd/03062019-163928

Laccone, F., Malomo, L., Froli, M., Cignoni, P., Pietroni, N.: Automatic design of cable-tensioned glass shells. Comput. Graph. Forum **39**(1), 260–273 (2020). https://doi.org/10.1111/cgf.13801

Liu, Q., Huang, X., Liu, G., Zhou, Z., Li, G.: Investigation on flexural buckling of laminated glass columns under axial compression. Eng. Struct. **133**, 14–23 (2017). https://doi.org/10.1016/j.engstruct.2016.12.006

López-Aenlle, M., Pelayo, F., Ismael, G., Prieto, M.G., Rodríguez, A.M., Fernández-Canteli, A.: Buckling of laminated-glass beams using the effective-thickness concept. Compos. Struct. **137**, 44–55 (2016). https://doi.org/10.1016/j.compstruct.2015.11.014

Louter, C., Belis, J., Veer, F., Lebet, J.P.: Structural response of SG-laminated reinforced glass beams; experimental investigations on the effects of glass type, reinforcement percentage and beam size. Eng. Struct. **36**, 292–301 (2012). https://doi.org/10.1016/j.engstruct.2011.12.016

Ludwig, J.J., Weiler, H.U.: Tragstrukturen aus Glas am Beispiel einer Ganzglastonne-Schalenkonstruktion ohne tragende Stahlunterkonstruktion am Maximilianmuseum in Augsburg. Bautechnik **77**(4), 246–249 (2000). https://doi.org/10.1002/bate.200001880

Luible, A., Schärer, D.: Lateral torsional buckling of glass beams with continuous lateral support. Glass Struct. Eng. **1**(1), 153–171 (2016). https://doi.org/10.1007/s40940-016-0008-3

Martens, K., Caspeele, R., Belis, J.: Development of composite glass beams-a review. Eng. Struct. **101**, 1–15 (2015a). https://doi.org/10.1016/j.engstruct.2015.07.006

Martens, K., Caspeele, R., Belis, J.: Development of reinforced and posttensioned glass beams: review of experimental research. J. Struct. Eng. **142**(5), 04015173 (2015b). https://doi.org/10.1061/(ASCE)ST.1943-541X.0001453

Martens, K., Caspeele, R., Belis, J.: Load-carrying behaviour of interrupted statically indeterminate reinforced laminated glass beams. Glass Struct. Eng. **1**(1), 81–94 (2016). https://doi.org/10.1007/s40940-016-0017-2

Mesnil, R., Douthe, C., Baverel, O.: Non-standard patterns for gridshell structures: fabrication and structural optimization. J. Int. Assoc. Shell Spat. Struct. **58**(4), 277–286 (2017). https://doi.org/10.20898/j.iass.2017.194.893

Neugebauer, J.: Applications for curved glass in buildings. J. Facade Des. Eng. **2**(1–2), 67–83 (2014). https://doi.org/10.3233/FDE-150016

Pottmann, H.: Architectural Geometry, vol. 10. Bentley Institute Press, Crewe (2007)

Romme, Sørvin, A., Bagger, I., Anne: Spaceplates building system. In: Cruz, P.J.D. (ed.) Structures and Architecture: Concepts, Applications and Challenges, pp. 1401–1408. CRC Press (2013)

Santarsiero, M., Bedon, C., Moupagitsoglou, K.: Energy-based considerations for the seismic design of ductile and dissipative glass frames. Soil Dyn. Earthq. Eng. **125**, 105710 (2019). https://doi.org/10.1016/j.soildyn.2019.105710

Schlaich, J., Schober, H.: Glass-covered grid-shells. Struct. Eng. Int. **6**(2), 88–90 (1996). https://doi.org/10.2749/101686696780495716

Timm, C., Chase, J.: Thermally curved glass for the building envelope. In: Challenging Glass 4 & COST Action TU0905 Final Conference, p. 141. CRC Press (2014)

Timoshenko, S.P., Gere, J.M.: Theory of Elastic Stability. Courier Corporation, Chelmsford (2012)

Veer, F.A., Wurm, J., Hobbelman, G.J.: The design, construction and validation of a structural glass dome. In: Proceedings of the Glass Processing Days. Poster, 12, vol. 12 (2003)

Villiger, J., Willareth, P., Doebbel, F., Nardini, V.: Interlocking glass spiral as building structure of the watch museum "La Maison des Fondateurs". Glass Struct. Eng. **4**(1), 3–16 (2019). https://doi.org/10.1007/s40940-018-0077-6

Wang, X., Feng, Rq, Yan, Gr, Liu, Fc, Xu, Wj: Effect of joint stiffness on the stability of cable-braced grid shells. International Journal of Steel Structures **16**(4), 1123–1133 (2016). https://doi.org/10.1007/s13296-016-0041-8

Weller, B., Reich, S., Ebert, J.: Testing on Space Grid Structures with Glass as Compression Layer. In: Proceedings of the Challenging Glass Conference, Delft, pp. 155–162 (2008)

Wurm, J.: Glass Structures, Design and Construction of Self-supporting Skin. Birkhäuser, Berlin (2007)